

Molecular dynamics simulations of fine structure in oxygen *K*-edge x-ray emission spectra of liquid water and ice

Michael Odelius

FYSIKUM, Stockholm University, Albanova, S-106 91 Stockholm, Sweden

(Received 26 August 2008; revised manuscript received 11 March 2009; published 16 April 2009)

X-ray emission (XE) spectroscopy has recently been taken as evidence for specific molecular structures in hydrogen bonded liquids. Experimentally derived and contradicting interpretations of the fine structure in the XE spectra of liquid water have been proposed in the literature. Here it is shown that all features of the XE spectra of liquid water can be explained based on *ab initio* molecular dynamics simulations by including core-hole excited-state dynamics. Future experiments are proposed which could discriminate between existing interpretations without relying on theory.

DOI: 10.1103/PhysRevB.79.144204

PACS number(s): 82.50.Kx, 34.50.Gb, 78.70.En, 82.53.Uv

I. INTRODUCTION

Experimental techniques to probe the electronic structure of complex systems can be used to derive information on chemical bonding and molecular structure and constitute a natural linkage to electronic structure calculations. X-ray emission (XE) spectroscopy is an important complement to photoelectron spectroscopy¹⁻³ for probing the local density of states of occupied states in complex systems which enables element specificity and through resonant inelastic x-ray scattering also chemical specificity. The XE process for oxygen occurs as a result of fluorescence decay of the core-hole created by exciting an O[1s] core electron to the unoccupied states by oxygen *K*-edge x-ray absorption. The transition moment projects out the local density of states around the core-excited atom. Fluorescence is the minority (<1%) decay channel for core holes in low-*Z* elements such as oxygen, but it is more easily related to electronic structure calculations than the dominant Auger decay which involves doubly ionized states.

Recent experimental development has made it possible to measure x-ray emission spectra in liquid systems.⁴⁻¹³ The spectral features in the XE spectrum of liquid water is in close analogy with the photoelectron spectrum,^{3,14} which contains a sharp lone-pair feature at high emission energy from the nonbonding out-of-plane $1b_1$ state, the bonding $3a_1$ state broadened predominantly through electronic mixing by intermolecular interaction and the bonding $1b_2$ state broadened by the distribution of O-H bond distances. For hydrogen(H)-bonded liquids, such as water, methanol, ethanol, and mixtures thereof, the high-resolution XE spectra contain fine structure, which is not observed with photoelectron spectroscopy.^{3,14} The fine structure has been ascribed to specific molecular structures in the liquid phase.^{4-7,13}

However, it has been shown through isotope substitution experiments and *ab initio* molecular dynamics (MD) simulations,^{8,9} that O 1s XE spectra of H-bonded liquids can be strongly influenced by excited-state dynamics occurring during the finite core-hole lifetime.^{15,16} Ultrafast (<10 fs) bond dissociation occurs in the core-excited state and can be selectively controlled by tuning the excitation energy,^{8,9} since long-lived (>20 fs) electron localization occurs for resonant excitations into the pre-edge of the x-ray absorption

spectrum.¹⁷ As a consequence, the XE spectrum is the result of spectral evolution and spectral features merge into the lone-pair peak as the molecule dissociates into OH or O species.

For liquid water, the fine structure in the high-resolution XE spectrum was recently ascribed on solely experimental grounds to such dynamical processes.^{10,11} This interpretation was later challenged in a study¹³ in which the fine structure instead, based on both experimental and theoretical analyses, was taken as evidence of a two-component mixture model of liquid water with classes of molecules in distinctly different H-bond environment.

The particular feature mainly under debate in the XE spectrum of liquid water is the splitting of the oxygen lone-pair into two sharp peaks at high emission (low-binding) energy seen in the experimental nonresonant XE spectra in Fig. 1. This splitting was not completely resolved in earlier

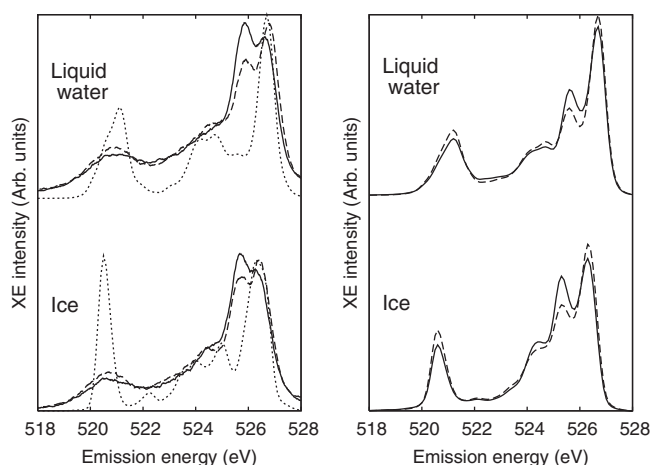


FIG. 1. The isotope effect in the x-ray emission spectra for ice and liquid water. H₂O (solid lines) and D₂O (dashed lines). Left: The experimental XE spectra of liquid water at 7 °C and amorphous ice from Tokushima *et al.* (Ref. 13) are compared to the simulated XE(*t*=0) spectra (dotted lines) excluding the effect of core-hole excited-state dynamics i.e., at time zero in the excited-state evolution presented in Figs. 2 and 3. Right: the simulated XE spectra for liquid water (top) and ice (bottom) including the effect of core-hole excited-state dynamics.

data^{4,5,9} but similar features have been detected for simple alcohols.^{6,7}

In favor of a dynamical interpretation of the fine structure,^{10,11} the present simulations of XE in liquid water show that *ab initio* molecular dynamics simulations can qualitatively reproduce the experimental XE spectra.

In the paper, I describe the computational approach and present results on the nonresonant XE spectra of liquid water and ice. I compare to available experimental and theoretical data and propose new experiments which could discriminate between the two different interpretations without relying on theoretical support. In the Appendix, I present more approximate simulations of the resonant XE spectrum for excitation into the x-ray absorption pre-edge.

II. METHODS

The simulation of the XE spectrum is based on density-functional calculations (DFT) and a classical approach which involves short (20 fs with 0.5 fs time step) MD simulations of the evolution in the core-hole excited state followed by XE spectrum simulations (every femtosecond) along the excited-state trajectory.^{8,9} The calculated discrete spectra are convoluted with a Gaussian function (0.4 eV full-width half-maximum) which entails the lifetime broadening (0.18 eV) and the instrumental broadening (0.35 eV) and finally weighed together according to an exponential decay mechanism.

The initial conditions for the excited-state Born-Oppenheimer dynamics are sampled over the ground-state Car-Parrinello MD simulation. The sampling is performed over all oxygen atoms a snapshot in a room-temperature Car-Parrinello MD simulation consisting of 64 water molecules performed with the CPMD code¹⁸ using a gradient-corrected density functional, BLYP (Refs. 19 and 20) and a 85 Ry kinetic-energy cutoff for the plane-wave expansion of the Kohn-Sham wave functions. For hydrogen a local pseudopotential parametrized with one Gaussian was used.²¹ The pseudopotential for oxygen was of Troullier-Martins type²² expressed in the Kleinman-Bylander form,²³ for core-excited oxygen is represented by a $O[1s^1]$ pseudopotential.^{8,9}

The excited-state dynamics is performed on clusters of 17 water molecules²⁴ centered around the core-excited oxygen, but the results are stable with respect to system size. Simulations performed on the full periodic system with a 0.1 fs time step showed only small geometric differences to the cluster simulations.

The XE spectra are simulated with the STOBE code²⁴ using the same computational framework as in previous publications,⁹ with the essential difference that the energy scale of the XE spectra is corrected in a Δ Kohn-Sham approach. The XE spectra are generated from clusters of 32 water molecules, but an energy correction for the emission energy of the out-of-plane lone-pair $1b_1$ state is obtained from the corresponding 17 water molecule clusters. In an Δ Kohn-Sham calculation, the total-energy difference between the core-ionized and the lone-pair valence-ionized state is used as an accurate determination of the emission energy for the state of interest, and to shift each XE spectrum.

The metastable core-ionized state is easily optimized due to the small overlap between core and valence orbitals. The lone-pair valence-ionized state, however, requires an approximate treatment based on a sequence of calculations in which the wave function is partially optimized. The isolated water molecule is used to define a subspace of five occupied molecular orbitals (MO) within the 17 molecule cluster. The electronic structure of the cluster is then optimized in the presence of the full core hole without allowing for mixing between the five MO subspace and the remaining orbitals, which relaxes the electronic structure of the surrounding water molecules. Finally the total energy of the valence-ionized state of the excited water molecule in the cluster is determined by a constrained wave-function optimization disallowing mixing with the remaining occupied orbitals. This procedure was calibrated on small clusters in which symmetry could be used to put the valence hole in the out-of-plane lone-pair $1b_1$ state and was accurate within 0.1 eV. (A similar procedure for the core-ionized state perfectly reproduces the fully optimized energy.)

The final comparison to the experimental data involves an exponential averaging of the XE spectrum along the excited-state trajectory.^{8,9} with a lifetime of 3.6 fs for the core hole.¹⁶ The isotope effect is approximately simulated by the using an effectively shorter lifetime (2.55 fs) in the exponential averaging of the nondeuterated trajectory to generate the XE spectra for a deuterated sample. For the isolated water molecule, comparison to experiment shows that the DFT calculation underestimate emission energy by 0.7 eV, which consequently is used as an additional correction through out the paper. For comparison to the XE spectrum simulations on liquid water, I also computed the spectra for cubic ice using the same 17 structural models as in Tokushima *et al.*¹³ Notice that the excited-state dynamics for the ice models was starting from the optimized geometries excluding initial velocities.

III. RESULTS

I sample the nonresonant XE spectra of liquid water over CPMD simulations to determine if the experimentally observed isotope effect can be explain on the basis of *ab initio* MD simulations alone or if a two-component model of liquid water is required. In the process, the excitation-energy dependence in the XE spectrum is also discussed and the XE spectrum for ice is simulated. In the presentation of the theoretical results, I will begin with evaluating the simulated nonresonant XE spectra for ice, then compare to the nonresonant XE spectra for liquid water. The present simulations are performed in close analogy with previous studies^{8,9} for liquid water at ambient conditions and for ice at zero Kelvin. The detailed theoretical basis and a preliminary study of the resonant XE spectrum are presented in the appendix.

Before analyzing the properly simulated XE spectra which includes the effect of a lifetime average over the core-hole excited-state dynamics, the experimental XE spectra for ice and liquid water are compared with the calculated “(time zero in excited-state dynamics) “XE($t=0$) spectra.” On the left-hand side of Fig. 1, the ground-state geometries do not

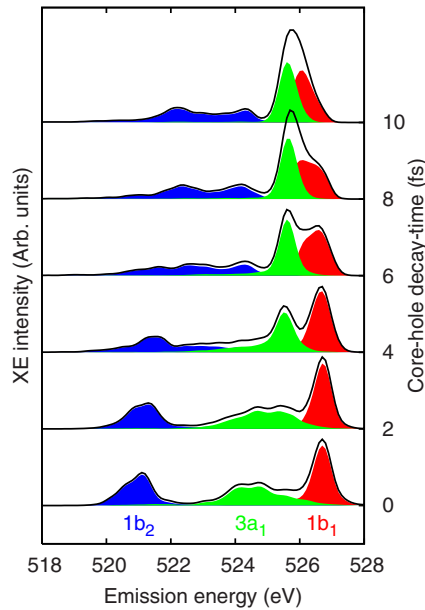


FIG. 2. (Color online) The evolution of the average XE spectrum along the core-hole excited-state dynamics in liquid water (H_2O). Symmetry decomposition is included. Total spectra (black lines), out-of-plane component (“ $1b_1$ ”), bisector component (“ $3a_1$ ”) and “H-H vector” component (“ $1b_2$ ”)

reproduce the experimentally observed lone-pair splitting in liquid water. Notice that these XE($t=0$) spectra differ from the simulation of photoelectron spectra,^{3,14} which are averaged on a binding energy scale. On an emission energy scale the $1b_1$ lone-pair peak is very sharp despite dynamical averaging since the shapes of the energy surfaces of core-ionized state and lone-pair valence-ionized state are similar for internal distortions of the water molecule and to some extent also intermolecular degrees of freedom.

From the experimental data in the literature,^{10,11,13,25} it is not established whether the XE spectrum for a perfect ice would show a splitting in the lone-pair peak at highest emission energy. The recent results for amorphous ice and multilayer ice films^{11,13} exhibit a splitting, but in previous experiments on ice²⁵ a temperature dependence related to structural disorder was observed.

On the right-hand side of Fig. 1, the simulated XE spectra for ice and liquid water, including the lifetime average over the core-hole excited-state dynamics are presented. A splitting in the lone-pair peak is clearly observed for all spectra, but the experimental intensity ratio between the peaks is not reproduced in particular not for ice. Furthermore, the width of the $1b_2$ peak at lowest emission energy is too narrow. The peak or shoulder at 524.5 eV from the $3a_1$ state is more distinct in ice than in liquid water, just as in the experiment. Overall, specific fine structures in the experimental XE spectra of both ice and liquid water are reproduced, although the intensities and line widths are not in quantitative agreement.

The spectral evolution along the core-hole excited-state dynamics, used in the generation of the XE spectra in Fig. 1, is presented in Figs. 2 and 3. By sampling the spectra in the molecular frame, the spectral components in different orbital symmetries can be followed. (The gas phase C_{2v} symmetry

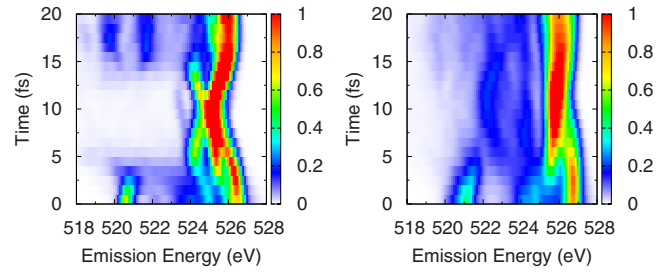


FIG. 3. (Color online) Two-dimensional representation of the spectral evolution along the core-hole excited-state dynamics (H_2O) used in generation of XE spectra in Fig. 1. The spectral intensity is on an arbitrary intensity scale. Left: ice; Right: Liquid water.

classes are used despite the fact that the molecular symmetry is broken by the environment and the excited-state dynamics.) The coordinate system of the each excited molecule is calculated from the out-of-plane and bisector directions of the O-H vectors, and the resulting orthogonal direction is approximately along the H-H vector.

From Fig. 2, I conclude that the splitting in the lone-pair peak is not of pure $1b_1$ symmetry but the double peak feature rather consists of two peaks of different symmetry; $3a_1$ and $1b_1$. The $3a_1$ component exhibits strong changes from an intact water molecule due to ultrafast dissociation into OH or O.^{8,9} In the sampling a broad range of dissociation events occur, but the net effect is a split lone-pair peak. The spectral evolution is also presented in Fig. 3. Apart from the evolution of the $1b_1$ lone-pair peak and rises in the $3a_1$ (and to some extent $1b_2$) lone-pair peaks giving rise to the split lone pair, one can also understand why the peak at 524.5 eV in ice is much sharper than in liquid water. According to the simulations, this peak is of $1b_2$ character and not of $3a_1$ character as would be inferred from its energy position.

Having assigned the splitting of the lone-pair peak in the XE spectrum of liquid, the next step is to understand the reasons for the lack of lone-pair splitting for excitations into the x-ray absorption pre-edge of liquid water. In the Appendix it is shown that the single lone-pair peak in the resonant XE spectrum for pre-edge excitations is due to the spectral response to a different core-hole dynamics.

IV. DISCUSSION

My conclusion from the nonresonant XE spectra for ice and liquid water and the resonant XE spectra for liquid water is that *ab initio* molecular dynamics simulations can qualitatively reproduce the experimental XE spectra without reference to a two-component model of liquid water. Distinct features and differences in the experimental XE spectra are captured by the simulation, but there are also important discrepancies. Most importantly, there is a mismatch in intensity ratio for the lone-pair peaks, and the $1b_2$ peak is too narrow in all spectra in Fig. 1. I ascribe these two deficiencies to the limitations of the classical MD treatment.

The width of the $1b_2$ peak directly reflects the distribution of internal O-H bond length, which is much too narrow in a classical simulation. As concluded in studies of Auger spec-

tra of water,²⁶ a classical treatment will also slow down the dissociation in the excited state. As can be deduced from Fig. 3, the speed of the dissociation strongly influences the ratio of the $1b_1$ and $3a_1$ lone-pair peaks via the lifetime average of the XE spectra. A quantitative simulation of the XE spectra would require a quantum dynamical treatment but in combination with the configurational sampling even a semiclassical approximation would result in a tremendous computational effort. Further theoretical studies, preferably including quantum dynamics, are necessary to study in detail the excitation-energy dependence in the XE spectra of liquid water and its temperature dependence.

In the present paper, *ab initio* MD simulations and XE spectrum simulations are performed on the level of classical approximation to try to decide between the two interpretations of the XE spectrum of liquid water^{10,11,13} and to determine if the claims about the molecular structure in liquid water/alcohols are valid.⁴⁻⁷ For this purpose it is essential to perform extensive sampling over different initial conditions and in the sampling to weigh together the simulated XE spectra on an accurate (relative) energy scale. I want to stress that these results are obtained by unbiased sampling over structures from a classical (as opposed quantum dynamical) *ab initio* MD simulation model. The simulations show that the classical core-hole dynamics can result in distinct sharp spectral features, not related to ground-state structures.

As derived from the classical approximation, the finite core-hole dynamical effect is sampled in real time by a lifetime averaging over classical core-hole excited-state trajectories with the initial conditions taken from a classical CPMD simulation. The procedure for spectrum simulations is very similar to that in the study of Tokushima and co-workers^{13,27} The second-most importance difference is the Δ Kohn-Sham correction that I employ to obtain an accurate energy scale, which results in a more well-defined lone-pair splitting without altering the basic interpretation. However, the decisive difference lies in the initial conditions for the excited-state dynamics.

Tokushima and co-workers^{13,27} developed an unorthodox method to include quantum effects in the spectrum simulations through classical simulations with peculiar initial conditions. In configurations from a classical ground-state MD simulation, the excited-state dynamics was initialized with the OH stretches at their equilibrium positions and classical velocities corresponding to the zero-point energy (1800 cm^{-1}) on the core-excited water molecule. Their initial conditions, with the OH stretches at the potential minimum and huge velocities, clearly correspond to an unphysical situation much less representative for the proper quantum distribution, than the rigorous classical approach employed in the present simulations. The unphysical initial conditions for the excited-state dynamics led to an artificial smearing of the lone-pair peak in the XE spectrum. Hence, an incorrect conclusion was drawn by Tokushima and co-workers^{13,27} that excited-state dynamics could not be the cause of the lone-pair splitting, which could only arise from the existence of two distinct classes of water molecules.

Ideally one would like to decide between the two interpretations of the fine structure in the XE spectrum for liquid water^{10,11,13} without relying on theory. This can be accom-

plished by measuring the angular anisotropy in the XE spectrum to determine the symmetry character of the two lone-pair peaks on solely experimental grounds.

Imagine an experiment in which the water molecules are resonantly excited by x rays from the X direction in the laboratory frame and linearly polarized in the Z direction, after which the detector is placed in the X , Y , or Z direction. Ideally only a particular polarization of the emitted x rays would be measured, but even without this possibility the experiments would be decisive. For resonant excitations in the x-ray absorption spectrum, water molecules with particular orientations in the laboratory frame will predominantly be excited. In a symmetric H-bond environment, the postedge (or pre-edge) state is dominated by the $2b_2$ (or $4a_1$) state, and molecules with the H-H vector (or molecular dipole) oriented along the Z direction are preferentially probed. As a consequence, for the detection in the Y direction, and if only Z -polarized x rays were detected, the $2b_2$ (of $4a_1$) component would be enhanced in the XE spectrum. This would determine if the split lone-pair peak consists of peaks with different origin. Different resonant excitations will yield variations in the dynamical response in the excited state, but for post-edge excitations the response is similar to nonresonant excitations and the electron delocalization is anyhow very fast.¹⁷

The proposed experiment might be complicated in liquid water by strong asymmetries in the H-bond donation, which would result in mixing of the $2b_2$ and $4a_1$ states. However, in ice a symmetric H-bond environment is guaranteed, and the peak at 524.5 eV in the XE spectrum of ice could be used to evaluate the present results. The simulations predict this peak to unexpectedly be of $2b_2$ character, and enhanced for excitations into the x-ray absorption postedge under the experimental conditions discussed above.

It has recently come to my knowledge that the angular anisotropy in resonant inelastic soft x-ray scattering of liquid water has been measured for pre-edge and main-edge excitations.²⁸ The two sharp lone-pair peaks are shown to be of different symmetry, which is not compatible with the two-component interpretation, since that implies that the lone-pair peak both are of b_1 symmetry. The present theoretical results, however, explain how the observed angular anisotropy can arise from excited-state dynamics during the finite core-hole lifetime.

ACKNOWLEDGMENTS

This work was supported by the Swedish Research Council (VR) and performed on the Swedish National Supercomputer Center (NSC) and Center for Parallel Computing (PDC), Sweden. I gratefully acknowledge O. Takahashi, who performed part of the calculations at the Information Media Center at Hiroshima University and Research Center for Computational Science, Okazaki, Japan.

APPENDIX: RESONANT X-RAY EMISSION SPECTRA

Experimentally the excitation-energy dependence in the resonant XE spectra¹⁰⁻¹³ has been measured, and since the splitting in the lone-pair peak disappears for resonant pre-

edge excitations in liquid water, it would be very interesting to perform an equally careful sampling of the resonant XE spectrum. However, the calculated XE spectra for resonant pre-edge excitations are much more uncertain than the non-resonant XE spectra for two important reasons.

(1) The pre-edge peak in the x-ray absorption spectrum of liquid water has been assigned to water molecules with at least one weakly H-bond donating OH group, but exact geometric criteria for the pre-edge feature depends strongly on the details in the spectrum simulations and is under intense debate.^{29–32} Hence, the weight in the resonant XE spectrum for each configuration is far from uncontroversial.

(2) Moreover, the excited-state dynamics and the XE spectrum calculations should be performed in the presence of the core-excited electron, the latter of which was not possible with the present energy-scale correction.

Nevertheless, a simplistic procedure was designed to get a qualitative picture of the resonant XE spectrum. This was desirable since the disappearance of the lone-pair splitting needs an explanation also in the simulation framework. The core-hole dynamics after resonant excitation can be performed in the lowest core-excited state, which profoundly influences the ultrafast bond dissociation for asymmetrically H-bonded water molecules.^{8,9} An additional energy shift of -0.7 ± 0.3 eV for resonant XE spectra was estimated by Δ Kohn-Sham calculation on the core-hole state the highest valence-ionized state in the full periodic system, but the XE spectra were calculated as for the nonresonant XE spectra but along the trajectory of the resonant core-excitation dynamics.

Finally, the resonant XE spectra are simulated by selecting a few configurations with strong x-ray absorption pre-edge intensity, as calculated with the transition potential method.^{29,30} These four cases were in single H-bond donor configurations where the excited water molecule has one OH group involved in strong H-bonding and a weak or nonexisting H-bond on the other OH group. In the nonresonantly core-excited state, these configurations undergo dissociation of the H-bonded OH group whereas after resonant pre-edge excitation the uncoordinated OH group dissociates, which as noticed previously⁹ gives a different spectral evolution. In order to separate differences in spectral response to the

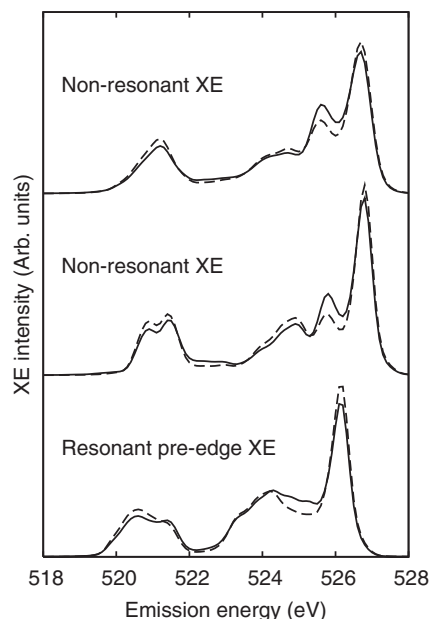


FIG. 4. Excitation energy dependence in the XE spectrum of liquid water. The isotope effect H_2O (solid lines) and D_2O (dashed lines) is included. Top: nonresonant XE spectra averaged over all water molecules. Bottom: resonant (lowest core-hole excited-state) XE spectra averaged over the four configurations corresponding to significant x-ray absorption pre-edge. Middle: nonresonant XE spectra averaged over the same four configurations.

excited-state dynamics from differences related to sampling, the resonant XE spectra in Fig. 4 are compared to the non-resonant XE spectra both from all configuration and from the restricted sampling over the same four configurations. The nonresonant XE spectra in Fig. 4 are not strongly affected by the restricted sampling, which also shows a splitting in the lone-pair peak at 525.5–526.5 eV. The resonant XE spectra do not exhibit the lone-pair splitting, since the $3a_1$ component does not evolve into a sharp feature and the binding orbitals ($1b_2$ and $3a_1$ components) tend to shift more along the excited-state dynamics.

¹J.-E. Rubensson, J. Electron Spectrosc. Relat. Phenom. **92**, 189 (1998).

²See various articles in Journal of Electron Spectroscopy and Related Phenomena 110/111 (2000).

³B. Winter, R. Weber, W. Widdra, M. Dittmar, M. Faubel, and I. Hertel, J. Phys. Chem. A **108**, 2625 (2004).

⁴S. Kashtanov, A. Augustsson, Y. Luo, J.-H. Guo, C. S  the, J.-E. Rubensson, H. Siegbahn, J. Nordgren, and H.   gren, Phys. Rev. B **69**, 024201 (2004).

⁵J.-H. Guo, Y. Luo, A. Augustsson, J.-E. Rubensson, C. S  the, H.   gren, H. Siegbahn, and J. Nordgren, Phys. Rev. Lett. **89**, 137402 (2002).

⁶J.-H. Guo, Y. Luo, A. Augustsson, S. Kashtanov, J.-E. Rubens-

son, D. K. Shuh, H.   gren, and J. Nordgren, Phys. Rev. Lett. **91**, 157401 (2003).

⁷S. Kashtanov, A. Augustsson, J.-E. Rubensson, J. Nordgren, H.   gren, J.-H. Guo, and Y. Luo, Phys. Rev. B **71**, 104205 (2005).

⁸B. Brena, D. Nordlund, M. Odellius, H. Ogasawara, A. Nilsson, and L. G. M. Pettersson, Phys. Rev. Lett. **93**, 148302 (2004).

⁹M. Odellius, H. Ogasawara, D. Nordlund, O. Fuchs, L. Weinhardt, F. Maier, E. Umbach, C. Heske, Y. Zubavichus, M. Grunze, J. D. Denlinger, L. G. M. Pettersson and A. Nilsson, Phys. Rev. Lett. **94**, 227401 (2005).

¹⁰O. Fuchs, F. Maier, L. Weinhardt, M. Weigand, M. Blum, M. Zharnikov, J. Denlinger, M. Grunze, C. Heske, and E. Umbach, Nucl. Instrum. Methods Phys. Res. A **585**, 172 (2008).

- ¹¹O. Fuchs, M. Zharnikov, L. Weinhardt, M. Blum, M. Weigand, Y. Zubavichus, M. Bär, F. Maier, J. D. Denlinger, C. Heske, M. Grunze and E. Umbach, *Phys. Rev. Lett.* **100**, 027801 (2008).
- ¹²O. Fuchs, M. Zharnikov, L. Weinhardt, M. Blum, M. Weigand, Y. Zubavichus, M. Bär, F. Maier, J. D. Denlinger, C. Heske, M. Grunze and E. Umbach, *Phys. Rev. Lett.* **100**, 249802 (2008).
- ¹³T. Tokushima, Y. Harada, O. Takahashi, Y. Senba, H. Ohashi, L. G. M. Pettersson, A. Nilsson, and S. Shin, *Chem. Phys. Lett.* **460**, 387 (2008).
- ¹⁴D. Nordlund, M. Odelius, H. Bluhm, H. Ogasawara, L. G. M. Pettersson, and A. Nilsson, *Chem. Phys. Lett.* **460**, 86 (2008).
- ¹⁵O. Björneholm, A. Nilsson, A. Sandell, B. Hernnäs, and N. Mårtensson, *Phys. Rev. Lett.* **68**, 1892 (1992).
- ¹⁶F. Gel'mukhanov, H. Ågren, M. Neeb, J.-E. Rubensson, and A. Bringer, *Phys. Lett. A* **211**, 101 (1996).
- ¹⁷D. Nordlund, H. Ogasawara, H. Bluhm, O. Takahashi, M. Odelius, M. Nagasono, L. G. M. Pettersson, and A. Nilsson, *Phys. Rev. Lett.* **99**, 217406 (2007).
- ¹⁸(1997–2001), CPMD, Copyright IBM Corp 1990–2004, Copyright MPI für Festkörperforschung Stuttgart 1997–2001.
- ¹⁹A. D. Becke, *Phys. Rev. A* **38**, 3098 (1988).
- ²⁰C. Lee, W. Yang, and R. G. Parr, *Phys. Rev. B* **37**, 785 (1988).
- ²¹P. Giannozzi (unpublished).
- ²²N. Troullier and J. L. Martins, *Phys. Rev. B* **43**, 1993 (1991).
- ²³L. Kleinman and D. M. Bylander, *Phys. Rev. Lett.* **48**, 1425 (1982).
- ²⁴K. Hermann, L. G. M. Pettersson, M. E. Casida, C. Daul, A. Goursot, A. Koester, E. Proynov, A. St-Amant, and D. R. Salahub, *SToBe-deMon* version 2.2 (2006).
- ²⁵E. Gilberg, M. J. Hanus, and B. Foltz, *J. Chem. Phys.* **76**, 5093 (1982).
- ²⁶O. Takahashi, M. Odelius, D. Nordlund, A. Nilsson, H. Bluhm, and L. G. M. Pettersson, *J. Chem. Phys.* **124**, 064307 (2006).
- ²⁷L. G. M. Pettersson, T. Tokushima, Y. Harada, O. Takahashi, S. Shin, and A. Nilsson, *Phys. Rev. Lett.* **100**, 249801 (2008).
- ²⁸J. Forsberg, J. Gråsjö, B. Brena, J. Nordgren, L.-C. Duda, and J.-E. Rubensson, *Phys. Rev. B* **79**, 132203 (2009).
- ²⁹Ph. Wernet, D. Nordlund, U. Bergmann, M. Cavalleri, M. Odelius, H. Ogasawara, L. Å. Näslund, T. K. Hirsch, L. Ojamäe, P. Glatzel, L. G. M. Pettersson, and A. Nilsson, *Science* **304**, 995 (2004).
- ³⁰B. Hetenyi, F. D. Angelis, P. Gianozzi, and R. Car, *J. Chem. Phys.* **120**, 8632 (2004).
- ³¹J. D. Smith, C. D. Cappa, K. R. Wilson, B. M. Messer, R. C. Cohen, and R. J. Saykally, *Science* **306**, 851 (2004).
- ³²D. Prendergast and G. Galli, *Phys. Rev. Lett.* **96**, 215502 (2006).